



Missouri University of Science and Technology  
Scholars' Mine

Civil, Architectural and Environmental  
Engineering Faculty Research & Creative Works

Civil, Architectural and Environmental  
Engineering

01 Mar 2018

## Rupture of a Cryogenic Composite Overwrapped Pressure Vessel Following a High-Speed Particle Impact

William P. Schonberg

Missouri University of Science and Technology, [wschon@mst.edu](mailto:wschon@mst.edu)

Follow this and additional works at: [https://scholarsmine.mst.edu/civarc\\_enveng\\_facwork](https://scholarsmine.mst.edu/civarc_enveng_facwork)

 Part of the [Civil and Environmental Engineering Commons](#)

### Recommended Citation

W. P. Schonberg, "Rupture of a Cryogenic Composite Overwrapped Pressure Vessel Following a High-Speed Particle Impact," *Aerospace*, vol. 5, no. 1, MDPI AG, Mar 2018.

The definitive version is available at <https://doi.org/10.3390/aerospace5010020>



This work is licensed under a [Creative Commons Attribution 4.0 License](#).

This Article - Journal is brought to you for free and open access by Scholars' Mine. It has been accepted for inclusion in Civil, Architectural and Environmental Engineering Faculty Research & Creative Works by an authorized administrator of Scholars' Mine. This work is protected by U. S. Copyright Law. Unauthorized use including reproduction for redistribution requires the permission of the copyright holder. For more information, please contact [scholarsmine@mst.edu](mailto:scholarsmine@mst.edu).

Article

# Rupture of a Cryogenic Composite Overwrapped Pressure Vessel Following a High-Speed Particle Impact

William P. Schonberg

Civil, Architectural, and Environmental Engineering Department, Missouri University of Science & Technology, Rolla, MO 65409, USA; wschon@mst.edu

Received: 2 January 2018; Accepted: 14 February 2018; Published: 18 February 2018

**Abstract:** A primary spacecraft design consideration is the anticipation and mitigation of the possible damage that might occur in the event of an on-orbit micro-meteoroid or orbital debris (MMOD) particle impact. While considerable effort has been expended in the study of non-pressurized spacecraft components under room temperature conditions to MMOD impacts, technical and safety challenges have limited the number of tests that have been conducted on pressurized elements of such spacecraft, especially under cryogenic conditions. This paper presents the development of a data-driven equation for composite material pressure vessels under cryogenic operating conditions that differentiate between impact conditions that, given a tank wall perforation, would result in only a small hole or crack from those that would cause catastrophic tank failure. This equation would be useful to a spacecraft designer who might be able to tailor the design parameters and operating conditions of, for example, a fuel tank so that if such a tank were to be struck and perforated by the impact of an MMOD particle, then only a hole would occur and neither catastrophic spacecraft failure nor additional sizable debris would be created as a result of that impact.

**Keywords:** hypervelocity impact; cryogenic; COPV; rupture; orbital debris

---

## 1. Introduction

Most spacecraft have at least one pressurized vessel on board; for robotic spacecraft, it is usually a liquid propellant tank. In some satellite or spacecraft designs, the fuel tank or some other pressurized vessel is necessarily exposed to the hazards of space, including the micro-meteoroid and orbital debris (MMOD) environment. Because of the potential of serious mission-threatening damage that might result following an on-orbit MMOD impact, one of the primary design considerations of such spacecraft is the anticipation and mitigation of the possible damage that might occur in the event of such an impact.

Considerable energy and effort have been expended in the study of the response of non-pressurized spacecraft components under room temperature conditions to MMOD-like impacts. However, fuel tanks are pressurized internally and so their main walls will develop bi-axial stress fields because of that internal pressurization. Technical and safety challenges have limited the number of high-speed tests that have been conducted on the pressurized elements of such spacecraft, especially under cryogenic conditions.

In addition to a hole, it is possible that for certain tank designs, impact parameters, and operating conditions, a pressurized tank may experience catastrophic failure (i.e., a rupture) as a result of a hypervelocity impact. While a puncture and the resulting leak could result in the destabilization of the spacecraft's orbit, a tank rupture following an on-orbit MMOD impact could lead to loss of the spacecraft and quite possibly, for human missions, the loss of life. To perform risk assessments during the design phase of a spacecraft that consider and weigh the likelihoods and consequences of

the various failures that might occur following an on-orbit MMOD impact, equations are required that can discriminate between combinations of impact parameters and operating conditions that may or may not lead to a catastrophic failure event.

This paper presents the results of an effort directed at addressing one aspect of this problem, namely, the development of a general, data-driven equation for highly pressurized elements, such as fuel tanks, that would differentiate between the combinations of impact parameters and operating conditions that would result in only a small hole or crack from those that would cause catastrophic tank failure following a perforating high-speed impact event. This equation is an improvement over a previous version [1] in that the current version is comprised of unitless or non-dimensional terms, whereas the previous version was not. As a result, the equation developed herein is more amenable to incorporating additional, new impact test data and results for similar test conditions as they become available.

The developed equation is referred to as a rupture limit equation, or RLE, as it is constructed to distinguish between conditions resulting in either tank rupture or non-rupture. This is an important consideration in the design of a pressurized tank—if possible, design parameters and operating conditions should be chosen such that in the event of an on-orbit MMOD particle impact both spacecraft failure and the creation of additional sizable debris pieces (such as those that would be created in the event of tank rupture or catastrophic failure) are avoided.

The RLE presented herein is developed by applying multi-linear regression techniques to data obtained in earlier studies involving cryogenic composite overwrapped pressure vessels (COPVs) under high-speed impact loading conditions. This, then, is another improvement of the RLE presented herein over the previous version, which was, in effect, merely a hand-drawn or faired curve between two sets of data points. Since the equation in this paper is statistics based, it (and the statistics associated with it) can easily be included in a risk assessment analysis, whereas the previous version could not.

## 2. Data Overview

There have been many high-speed impact test studies performed using tanks or pressure vessels over the past 50 years. These tests have been performed with varying amounts of internal pressure (including none); with internal fluids, air, or at a vacuum; using metallic tanks and composite material tanks; with spherical tanks as well as cylindrical tanks; using internal fluids at temperatures ranging from room temperature to cryogenic temperatures; and, with and without MMOD shielding. Reference [2] provides a breakdown of the high-speed impact testing that has been performed using pressurized tanks over the past 50 years.

In this particular study, we focus on the high-speed impact tests performed on unshielded composite material overwrapped pressure vessels (COPVs) with internal cryogenic fluids. Data from these tests have been used to develop a rupture limit equation (or RLE) for these kinds of pressure vessels under these operating conditions. The purpose of this equation is to distinguish between impact parameters and operating conditions that would result in either only a small hole or crack (i.e., a non-rupture) from those that would cause catastrophic failure (i.e., a rupture).

The RLE is constructed using data from 24 impact tests—fifteen (15) were performed using so-called “pressure cylinders” (see Figure 1) while nine (9) of the tests were performed using “pressurized bottles” (see Figure 2). The pressure cylinders consisted of one flexible endcap plate made of the material of interest attached to a thick metal cylinder; impacts occurred along a line normal to the flexible endcap test specimen plate. The pressurized bottles consisted of a cylindrical test section to which heavy aluminum end closures were attached to form a closed tank; impacts occurred along a radial line normal to the cylindrical test section.

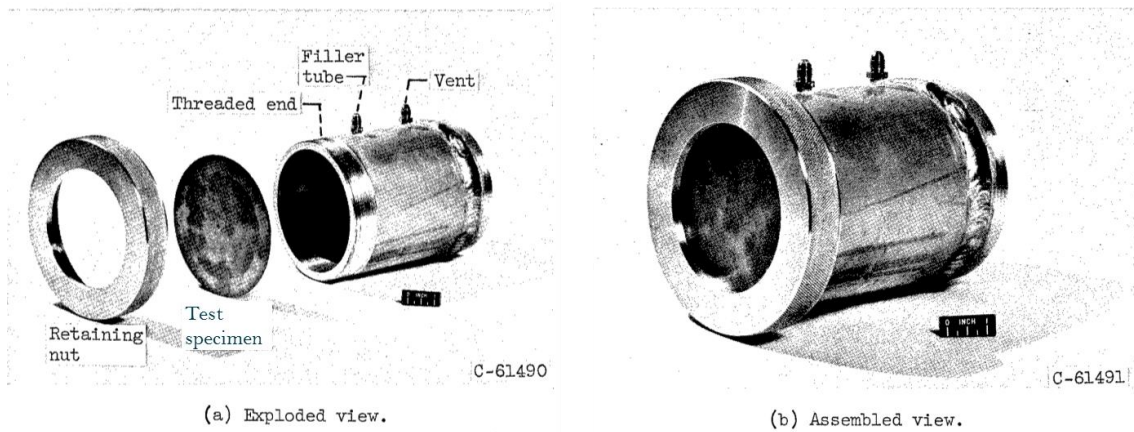


Figure 1. Pressure cylinder used in high-speed impact testing [3,4].

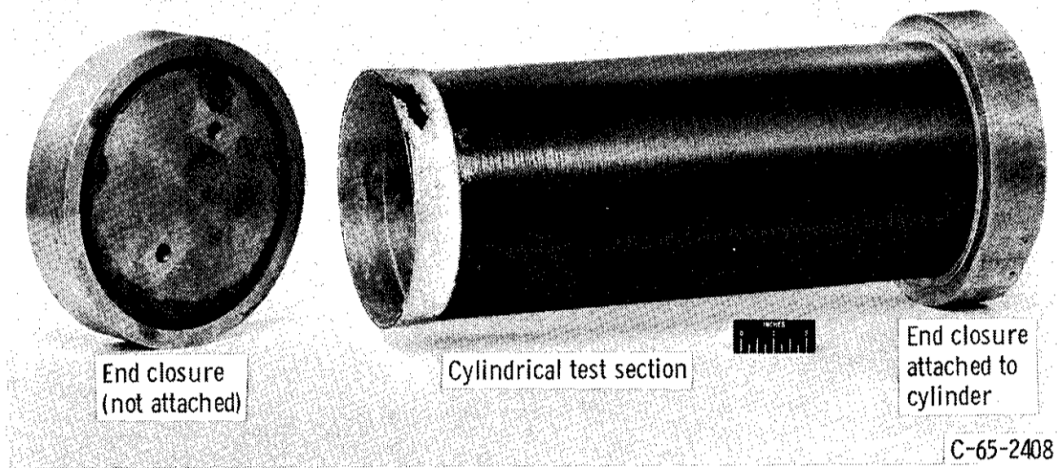


Figure 2. Pressurized bottle used in high-speed impact testing [4].

Tables 1–3 present a summary of the impact test conditions and the geometric parameters/material properties of the COPVs used in the development of the RLE, respectively.

Table 1. Overview of the impact test conditions.

| Parameter  | Reference [3]        | Reference [4]    | Units            |                    |
|------------|----------------------|------------------|------------------|--------------------|
| Projectile | Material             | Steel            | Steel            |                    |
|            | Density <sup>a</sup> | 7.8              | 7.8              | gm/cm <sup>3</sup> |
|            | Diameter             | 5.56             | 5.56             | mm                 |
| Trajectory | Obliquity            | 0                | 0                | deg                |
|            | Velocity             | 1.91             | 1.68             | km/s               |
| COPV       | Contents             | LOX <sup>b</sup> | LN2 <sup>c</sup> |                    |
|            | Temperature          | −300             | −330             | °F                 |
|            | Pressure             | 0                | ~0.34 to ~1.2    | MPa                |

<sup>a</sup> Nominal average density values from [www.matweb.com](http://www.matweb.com); <sup>b</sup> Liquid oxygen; <sup>c</sup> Liquid nitrogen.

**Table 2.** Geometric parameters and material properties of composite overwrapped pressure vessels (COPVs)—Reference [3].

| Parameter |                  |                   |                  |                      |                  |                     |                  | Units             |
|-----------|------------------|-------------------|------------------|----------------------|------------------|---------------------|------------------|-------------------|
| COPV Type |                  | Pressure Cylinder |                  |                      |                  |                     |                  |                   |
| Composite | Fiber Matrix     | Glass cloth Epoxy |                  | Nylon cloth Phenolic |                  | Dacron Polyurethane |                  |                   |
|           | Tensile Strength | 315 <sup>a</sup>  | 622 <sup>b</sup> | 75 <sup>a</sup>      | 119 <sup>b</sup> | 68 <sup>a</sup>     | 590 <sup>b</sup> | MPa               |
|           | Density          | 2.07 <sup>c</sup> |                  | 1.22 <sup>d</sup>    |                  | 1.30 <sup>d</sup>   |                  | g/cm <sup>3</sup> |
|           | Thickness        |                   |                  | 3.175                |                  |                     |                  | mm                |

<sup>a</sup> Nominal room temp composite strength values estimated from published component material room temperature strength values, <sup>b</sup> Calculated cryogenic composite or liner strength values, <sup>c</sup> Nominal composite density values from the manufacturer's literature, <sup>d</sup> Nominal composite density values estimated from published component material density values

The tests performed as reported in references [3,4] were motivated by a desire to understand the high-speed impact response of COPVs that were in use at the time when those studies were performed. The cryogenic strength values for the composite overwrap and liner materials used in those studies were not typically reported by the investigators of those studies, and so had to be estimated from corresponding room temperature strength values. In some cases, the required room temperature strength values could be found in the literature for composite materials similar in construction to those used in these studies. However, in others, room temperature strength values could not be found and had to be estimated using simple mixture theory and strength values for the component materials involved. The cryogenic strength values were then calculated using published information regarding changes in the strength values of the component materials as the ambient temperature was decreased to cryogenic conditions.

**Table 3.** Geometric parameters and material properties of COPVs—Reference [4].

| Parameter     |                  |                     |                   |                   |                   |                    |                  | Units                               |                                      |                   |
|---------------|------------------|---------------------|-------------------|-------------------|-------------------|--------------------|------------------|-------------------------------------|--------------------------------------|-------------------|
| COPV Type     |                  | Pressure Cylinder   |                   |                   |                   | Pressurized Bottle |                  |                                     |                                      |                   |
| COPV Diameter |                  | N/A                 |                   |                   |                   | 19.05              |                  | cm                                  |                                      |                   |
| Composite     | Fiber Matrix     | Steel wire Urethane |                   | Glass Urethane    |                   | Dacron Urethane    |                  | Glass Epoxy                         |                                      |                   |
|               | Tensile Strength | 137 <sup>a</sup>    | 1180 <sup>c</sup> | 205 <sup>a</sup>  | 1771 <sup>c</sup> | 68 <sup>a</sup>    | 590 <sup>c</sup> | 772 <sup>b</sup> –1407 <sup>b</sup> | 1016 <sup>c</sup> –1851 <sup>c</sup> | MPa               |
|               | Density          | 5.65 <sup>e</sup>   |                   | 2.03 <sup>e</sup> |                   | 1.30 <sup>e</sup>  |                  | 2.07 <sup>d</sup>                   |                                      | g/cm <sup>3</sup> |
|               | Thickness        |                     |                   | 0.508–1.60        |                   |                    |                  | 0.3–1.0                             |                                      | mm                |
| Liner         | Material         | None                |                   |                   |                   | Aluminum           |                  |                                     |                                      |                   |
|               | Tensile Strength | N/A                 |                   |                   |                   | 455 <sup>f</sup>   |                  | 523 <sup>c</sup>                    |                                      | MPa               |
|               | Shear Strength   | N/A                 |                   |                   |                   | 273 <sup>f</sup>   |                  | 314 <sup>c</sup>                    |                                      | MPa               |
|               | Yield Stress     | N/A                 |                   |                   |                   | 285 <sup>f</sup>   |                  | 328 <sup>c</sup>                    |                                      | MPa               |
|               | Density          | N/A                 |                   |                   |                   |                    |                  | 2.80 <sup>d</sup>                   |                                      | g/cm <sup>3</sup> |
| Thickness     | N/A              |                     |                   |                   |                   |                    | 0.127            |                                     | mm                                   |                   |

<sup>a</sup> Nominal room temperature composite strength values estimated from published component material room temperature strength values, <sup>b</sup> Nominal room temperature composite strength values provided in the cited reference, <sup>c</sup> Calculated cryogenic composite or liner strength values, <sup>d</sup> Nominal composite density values from the manufacturer's literature, <sup>e</sup> Nominal composite density values estimated from published component material density values, <sup>f</sup> Nominal room temperature liner strength values from [www.matweb.com](http://www.matweb.com).

### 3. Rupture Limit Equation Development

The empirically-based rupture limit equation (RLE) was developed using the rupture/non-rupture data from references [3,4]. To render the equation as broadly applicable as possible, the operating conditions ( $x$ -axis) were parameterized as the hoop stress in the tank (non-dimensionalized by the temperature-adjusted uni-axial ultimate tensile stress of the composite overwrap material), and the impact conditions ( $y$ -axis) were parameterized as the impact momentum (non-dimensionalized by a number of appropriate tank wall material properties). This approach was used successfully to



model the rupture/non-rupture response of cylindrical and spherical metallic tanks [2], as well as air-filled COPVs at room temperature [5] and flat composite plates [6] under high-speed impact loading conditions.

Following on the successful application of this approach in these previous studies, a simple power law form was chosen for the cryogenic COPV RLE to be developed herein. Specifically, the power law for the curve that is intended to separate the regions of rupture and non-rupture was chosen as follows:

$$\text{Non - dimensional Projectile Momentum} = A \left( \frac{\sigma_{hoop}}{\sigma_{ult}^{comp}} \right)^B \quad (1)$$

where  $\sigma_{hoop}$  and  $\sigma_{ult}^{comp}$  are the COPV hoop stress and uni-directional ultimate stress of the COPV composite material, respectively. In the case of the pressure cylinder tests, the COPV hoop stresses were taken as the stress values in the composite plate endcaps as given in references [3,4]. However, in the case of the pressurized bottle tests, the COPV hoop stresses were calculated using the equation:

$$\sigma_{hoop} = \frac{p_{int} r_{OD}}{t_{tot}} \quad (2)$$

where  $t_{tot} = t_{comp} + t_{liner}$  is the total nominal thickness of the COPV and is given by the sum of the thicknesses of the composite overwrap and liner (if any),  $p_{int}$  is the internal pressure in the COPV, and  $r_{OD}$  is the COPV outer radius.

In addition, the non-dimensional form of projectile momentum was taken to be as follows:

$$\text{Non - dimensional Projectile Momentum} = \frac{m_{proj} V_{proj}}{(\rho_{comp} t_{comp}^3) \sqrt{\frac{\sigma_{ult}^{comp}}{\rho_{comp}}}} \quad (3)$$

The first term in the denominator in Equation (3) has units of mass while the second has units of velocity, thereby rendering the right-hand side of Equation (3) unitless, or non-dimensional, so long as there is consistency in the units of mass and velocity used in its numerator and denominator.

To include the effects of other material parameters and the differences between the shapes of the cryogenic test articles, Equation (3) was modified through the addition of a number of other unitless terms, with the following result:

$$\text{Non - dimensional Projectile Momentum} = \frac{m_{proj} V_{proj}}{(\rho_{comp} t_{comp}^3) \sqrt{\frac{\sigma_{ult}^{comp}}{\rho_{comp}}}} P \left( \frac{\rho_{proj}}{\rho_{comp}} \right)^Q \left( \frac{460+T}{530} \right)^R \left( 1 + \frac{\sigma_{ult}^{liner}}{100} \right)^S \left( 1 + \frac{\sigma_{yld}^{liner}}{100} \right)^T \quad (4)$$

where  $T$  is the temperature of the cryogenic fluid (in °F), and the ultimate and yield stresses of the liner material,  $\sigma_{ult}^{liner}$  and  $\sigma_{yld}^{liner}$ , respectively, if there is a liner present (in MPa). The yield and ultimate stress values are divided by 100 so the terms involving these quantities can have a meaningful effect without being excessively large compared to the values of the other terms in the equation. Combining Equations (1) and (4) yields the final form of the RLE as follows:

$$\frac{m_{proj} V_{proj}}{(\rho_{comp} t_{comp}^3) \sqrt{\frac{\sigma_{ult}^{comp}}{\rho_{comp}}}} P \left( \frac{\rho_{proj}}{\rho_{comp}} \right)^Q \left( \frac{460+T}{530} \right)^R \left( 1 + \frac{\sigma_{ult}^{liner}}{100} \right)^S \left( 1 + \frac{\sigma_{yld}^{liner}}{100} \right)^T = A \left( \frac{\sigma_{hoop}}{\sigma_{ult}^{comp}} \right)^B \quad (5)$$

The coefficient  $P$  and the exponents  $Q$ ,  $R$ ,  $S$ , and  $T$  in Equation (4) were selected so as to allow, as much as possible, a natural separation between the rupture and non-rupture data points. This would, in turn, facilitate the development of an RLE that would, again, as much as possible, lie between those two regions. The attractiveness and benefit of this approach are that if additional test results were to become available, the values of  $P$ ,  $Q$ ,  $R$ ,  $S$ , and  $T$  in Equation (3) could again be adjusted to allow the

incorporation of the new rupture/non-rupture data and the subsequent development of a new RLE. To this end, Table 4 presents the values of the coefficient  $P$  and exponents  $Q$ ,  $R$ ,  $S$ , and  $T$  used in the non-dimensionalization scheme defined in Equation (4):

**Table 4.** Values of  $P$ ,  $Q$ ,  $R$ ,  $S$ , and  $T$  in the non-dimensionalization scheme.

| Exponent | Value                     |                             |
|----------|---------------------------|-----------------------------|
| $P$      | Pressurized Bottle<br>1.0 | Pressure Cylinder<br>0.0167 |
| $Q$      | 7.0                       |                             |
| $R$      | 1.0                       |                             |
| $S$      | −1.0                      |                             |
| $4T$     | −1.0                      |                             |

The constants  $A$  and  $B$  in Equation (1) are determined through a linear regression of the rupture/non-rupture data using the Levenberg–Marquardt algorithm [7]. This is a common algorithm for minimizing a function over the space of parameters of the function (i.e., in this particular case, the coefficients in a user-defined function). In addition to solving for the coefficients, this algorithm also provides statistical information that can be used to assess the “goodness of fit” of the regression results, as well as standard deviation curves for the regression model.

The actual regression exercise was performed by first creating a function  $Z$  that would take on values of +1 or −1 depending on whether a particular test resulted in either a rupture or a non-rupture. This function is derived from the linearized form of Equation (5) and written as follows:

$$Z = W_1 \ln(X) + W_2 \ln(Y) + W_3 \quad (6)$$

where  $Y$  is a non-dimensionalized projectile momentum and  $X$  is the non-dimensionalized hoop stress, respectively. It is actually, then, the constants  $W_1$ ,  $W_2$ , and  $W_3$  that are obtained through a regression of the test parameters given by  $X$  and  $Y$  against test results given by  $Z$  and represented by a +1 or a −1. Once  $W_1$ ,  $W_2$ , and  $W_3$  are obtained, setting  $Z = 0$  yields the desired RLE. Furthermore, when we set  $Z = 0$ , solving for  $Y$  gives the following expression for  $A$  and  $B$  in terms of the regression parameters  $W_1$ ,  $W_2$ , and  $W_3$ :

$$A = \exp\left(-\frac{W_3}{W_2}\right) \quad (7)$$

$$B = -\frac{W_1}{W_2} \quad (8)$$

Table 5 and Figure 3 contain the results of this exercise, namely, the coefficients  $W_1$ ,  $W_2$ , and  $W_3$ , the correlation coefficient  $R^2$ , the standard deviations of  $W_1$ ,  $W_2$ , and  $W_3$ , and the covariance matrix for  $W_1$ ,  $W_2$ , and  $W_3$ .

**Table 5.** Results of the regression exercise.

| Regression Parameter | Regression Value | Standard Deviation |
|----------------------|------------------|--------------------|
| $W_1$                | −3.2629          | 1.0158             |
| $W_2$                | −1.8108          | 0.6076             |
| $W_3$                | 3.8888           | 1.7344             |
| $R^2$                | 71.7%            |                    |

$$\begin{bmatrix} \text{Var}(W1) = 1.0318 & & SYM \\ \text{Covar}(W2, W1) = 0.5487 & \text{Var}(W2) = 0.3692 & \\ \text{Covar}(W3, W1) = -1.0740 & \text{Covar}(W3, W2) = -0.9472 & \text{Var}(W3) = 3.0083 \end{bmatrix}$$

**Figure 3.** Statistical information from the regression exercise.

From the information in Table 5 and Equations (7) and (8), we find that  $A = 8.5636$  and  $B = -1.8019$ . This completes the development of the RLE for the test data considered in this study. In the next section, we compare the predictions of the RLE against test data and offer comments on the utility and limitations of this RLE.

#### 4. Comparison with Empirical Results

Figure 4 shows plots of the RLE developed herein compared to experimental rupture/non-rupture results. This figure also shows plots of  $\pm$ one standard deviation curves and  $\pm$ two standard deviation curves about the RLE curve. The orange data points represent those tests that resulted in tank rupture, while the green data points show those that did not for both types of test specimen configurations.

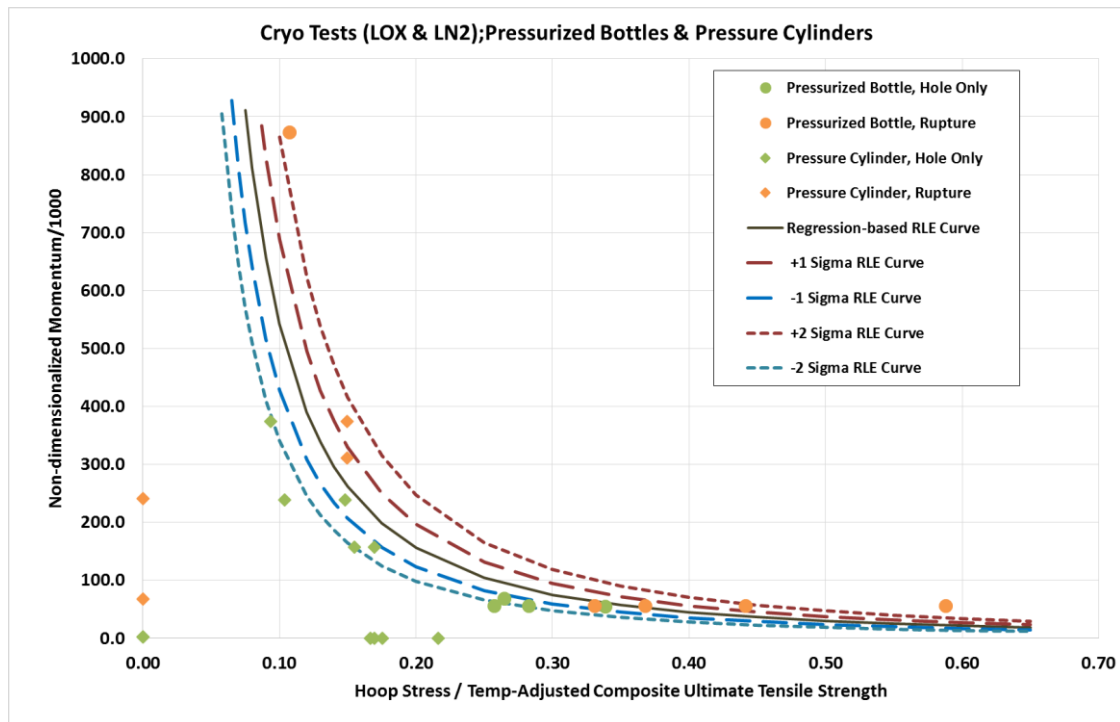


**Figure 4.** Plots of RLE (rupture limit equation) curve and experimental rupture/no-rupture data.

As can be seen in Figure 4, with the exception of the two ruptured unpressurized pressure cylinder tests, the RLE developed herein appears to predict fairly well the rupture/non-rupture response of COPVs at cryogenic temperatures. This is supported by the “tightness” of the confidence-bound curves about the RLE—another indication of the goodness of fit of the RLE to the rupture/non-rupture data. A possible explanation for the rupture of the two unpressurized cylinders is offered in reference [3]—namely, that the resins in these two tests had high percentages of organic polymeric matter. In the presence of liquid oxygen, this possibly made them highly susceptible to a catastrophic response, even without any internal pressure.

Of further note are the non-rupture points for several pressure cylinder tests that appear to lie on the  $x$ -axis (i.e., they appear to have a non-dimensional momentum value of zero, which would



correspond to a zero impact velocity). These points are actually not on the  $x$ -axis, just exceedingly close to allow comparison with the other non-rupture points.

Another means for assessing the ability of the RLE to discriminate between the region of impact parameters and operating conditions that would result in rupture from those that would not is through the use of specificity and sensitivity ratios. In the medical world, these values are frequently used to distinguish between false positives and false negatives. For example, if we designate a rupture event as the event we are testing for, then an actual rupture might be considered as a “positive reading,” while a non-rupture might be considered as a “negative reading.” As such, the following definitions could be applied to the demarcation line derived from the RLE developed herein:

$$\text{Sensitivity ratio} = (\text{Actual ruptures predicted as ruptures}) / (\text{Actual ruptures predicted as ruptures} + \text{Actual ruptures predicted as non-ruptures}) \quad (9)$$

$$\text{Specificity ratio} = (\text{Actual non-ruptures predicted as non-ruptures}) / (\text{Actual non-ruptures predicted as non-ruptures} + \text{Actual non-ruptures predicted as ruptures}) \quad (10)$$

These ratios yield a quantitative assessment of whether or not the RLE developed herein could be considered as conservative or non-conservative in the following manner:

- a low specificity value (i.e., many non-ruptures predicted as ruptures) and a high sensitivity value (i.e., fewer ruptures predicted as non-ruptures) → a conservative RLE
- a high specificity value (i.e., fewer non-ruptures predicted as ruptures) and a low sensitivity value (i.e., many ruptures predicted as non-ruptures) → a non-conservative RLE

Furthermore, if both values were found to be high, the RLE could be considered as fairly accurate, whereas if both values were low, that would indicate either a problem with the testing method or with test repeatability.

For the data considered herein and the RLE developed based on that data, we find that, even including the two ruptures that lie below the RLE curve, we have a sensitivity value of 0.78 and a specificity value of 0.93 (if the two “odd” rupture data points were removed, the sensitivity value would be exactly 1.0). Based on these results, we can again conclude that the RLE performs rather well in separating the test results where a rupture occurred from those that resulted in non-rupture.

It is important to note, of course, that there are a number of other parameters that can affect whether or not a COPV ruptures or merely sustains a hole following a high-speed impact event. This includes the filament winding pattern, the particular composite layup configuration, and the actual COPV contents (e.g., gas, liquid, or both), and others. These parameters were not considered in this investigation because the desire was to develop as simple an RLE as possible so that a user, for example, would not need to be concerned about knowing the particular layup configuration. As additional tests are performed and additional data made available, it is entirely possible that the RLE developed herein might need to be modified to take into account these and other parameters.

## 5. Concluding Thoughts

This paper presented a summary of the work performed to address a key issue related to the design of pressurized vessels and tanks that are part of a spacecraft that would be built to operate in the MMOD environment. An empirical equation was developed that would differentiate between impact parameters and operating conditions that would result in only a small hole or crack in a COPV with an internal cryogenic fluid from those that would cause catastrophic tank failure. This equation was found to be fairly adept in predicting the rupture/non-rupture response of pressurized COPVs at cryogenic temperatures. As such, it can be used alongside more detailed numerical and experimental efforts that are part of a comprehensive on-orbit risk assessment process.

**Acknowledgments:** The author wishes to extend his gratitude to the NASA Safety Engineering Center (NESC) for providing the support that made this study possible. The author also wishes to acknowledge the guidance and helpful suggestions of William E. Vesely (NASA HQ) during the course of the regression exercises in this investigation.

**Conflicts of Interest:** The author declares no conflict of interest.

## References

1. Schonberg, W.P. Predicting the Rupture of a Cryogenic Composite Pressure Vessel (COPV) Following a Hypervelocity Impact. Paper No. 166. In Proceedings of the 7th European Conference on Space Debris, Darmstadt, Germany, 18–21 April 2017.
2. Schonberg, W.P.; Ratliff, M. Hypervelocity Impact of a Pressurized Vessel: Comparison of Ballistic Limit Equation Predictions with Test Data and Rupture Limit Equation Development. *Acta Astronaut.* **2015**, *115*, 400–406. [[CrossRef](#)]
3. Dengler, R.P. *An Experimental Investigation of Chemical Reaction between Propellant Tank Material and Rocket Fuels or Oxidizers When Impacted by Small High-Velocity Projectiles*; NASA TN-D-1882; NASA Lewis Research Center: Cleveland, OH, USA, 1963.
4. Stepka, F.S. *Projectile-Impact-Induced Fracture of Liquid-Filled, Filament-Reinforced Plastic or Aluminum Tanks*; NASA TN-D-3456; NASA Lewis Research Center: Cleveland, OH, USA, 1966.
5. Schonberg, W.P. Rupture of Composite Pressure Vessels (COPVs) Following a Hypervelocity MMOD Particle Impact. Paper No. AIAA-2018-0231. In Proceedings of the AIAA SciTech Forum, Kissimmee, FL, USA, 8–12 January 2018.
6. Schonberg, W.P. A Rupture Limit Equation for Pre-Loaded Composite Plates. *J. Compos. Sci.* **2018**, *2*, 3. [[CrossRef](#)]
7. PSI Plot. *Scientific Spreadsheet and Technical Plotting User's Guide*; Poly Software International: Pearl River, NY, USA, 2010.



© 2018 by the author. Licensee MDPI, Basel, Switzerland. This article is an open access article distributed under the terms and conditions of the Creative Commons Attribution (CC BY) license (<http://creativecommons.org/licenses/by/4.0/>).